Efficiency and Emissions Measurement of a Stirling-Engine-Based Residential Microcogeneration System Run on Diesel and Biodiesel

Amir A. Aliabadi, Murray J. Thomson,* James S. Wallace, Tommy Tzanetakis,
Warren Lamont, and Joseph Di Carlo

*Department of Mechanical and Industrial Engineering, University of Toronto, 5 King's College Road,
Toronto, Ontario M5S 3G8, Canada*

Concern with climate change and energy security has generated interest in both cogeneration and biofuels. This experimental study examines the performance of a residential microcogeneration system based on a Stirling engine fueled by diesel and biodiesel. Run on diesel, the system achieves a power efficiency of 11.7% and a heat efficiency of 78.7%. The corresponding efficiencies for the system, when run on biodiesel, are slightly lower at 11.5% and 77.5%, respectively. Particulate emissions for biodiesel are 69.2 mg/kWh, an order of magnitude higher than that of diesel (2.3 mg/kWh). The total unburned hydrocarbon emissions for biodiesel are higher than those of diesel. Emissions of carbon monoxide, nitrogen dioxide, methane, acetylene, ethylene, formaldehyde, and acetaldehyde are comparable between diesel and biodiesel, but nitric oxide emissions for diesel are observed to be higher at 151 ppm compared to those for biodiesel (117 ppm). The difference in the performance of the system is generally attributed to higher boiling range compounds in biodiesel that affect the flame stability, the fuel evaporation, and the complete burnout of the fuel. The system achieves energy efficiencies comparable to those of internal-combustion-engine-based and fuel-cell-based cogeneration systems.

1. Introduction

1.1. Cogeneration. Cogeneration is the simultaneous production of more than one useful form of energy (such as power and heat).[1] This mode of operation often results in better utilization of the input energy source and offers many economic benefits. Residential microcogeneration systems can serve as an alternative to provide both electricity and heat to the residential sector by utilizing fossil fuels, primarily natural gas and diesel, more wisely. The energy converted using cogeneration systems will have lower greenhouse gas emissions than typical fossil fuel electricity generating stations and conventional residential furnaces combined. Also, if the power is consumed on site, transmission losses are avoided. Many new technologies have emerged that utilize the heat output even in microscale power. Current commercial systems provide power in the 0.5−1.5 kW range and heat in the 5.0−10.0 kW range, depending on the climate. The power is used directly or net metered via the grid, and the heat is used for space or domestic hot water heating.

1.2. Stirling Engines. Stirling engines can be economical sources of power when integrated into microcombined heat and power (micro-CHP) systems. There is much current interest in various CHP applications in residential, farming, and commercial facilities. Although the technology is not fully developed yet, it has a good potential to offer high efficiency, fuel flexibility, low emissions, low noise levels, low vibration levels, and good performance at partial load. In contrast with reciprocating internal combustion engines, the heat can be supplied from a variety of external sources, allowing the use of a wide range of fossil fuels, biomass, process heat, and solar energy. Stirling engines have low wear and long maintenance-free operating periods and are usually more quiet and smoother than reciprocating engines.[2]

The ideal Stirling cycle consists of four gas processes: an isothermal expansion (heat addition from the external source), a constant-volume regeneration (internal heat transfer from the working fluid to the regenerator), an isothermal compression (heat rejection to the external sink), and a constant-volume regeneration (internal heat transfer from the regenerator back to the working fluid).[3] In theory, Stirling engines are capable of reaching high thermal efficiencies, since, thermodynamically, they reach the Carnot efficiency in the ideal cycle. In practice, however, they exhibit much lower efficiencies due to material limitations (friction) and inefficient heat transfer (conduction). Current commercial Stirling engine thermal efficiencies range from 12% to 30%.[2]

Emissions from current Stirling engine burners can be 10 times lower than those of internal combustion (IC) engines based on Otto or Diesel cycles without catalytic converters. This makes emissions generated from Stirling engines comparable to those of modern gas burner technology. Stirling burners utilize air preheating to achieve a high combustion efficiency with low emissions. Sometimes the exhaust is mixed with the intake air to limit the maximum temperature, therefore suppressing the formation of nitrogen oxides. Also, Stirling burners feature a continuous combustion that considerably lowers the emission levels when compared to conventional IC-based cogeneration systems. The prominent emissions in Stirling engines are NO_x

---

* To whom correspondence should be addressed. Telephone: (416) 580-3391. Fax: (416) 978-7753. E-mail: thomson@mie.utoronto.ca.

(1) Çengel, Y. A.; Boles, M. A. *Thermodynamics: An Engineering Approach,* 4th ed.; McGraw-Hill Higher Education: New York, 2002; p 539.

(2) Onovwiona, H. I.; Ugursal, V. I. *Renewable Sustainable Energy Rev.* **2006,** *10,* 389–431.

(3) Çengel, Y. A.; Boles, M. A. *Thermodynamics: An Engineering Approach,* 4th ed.; McGraw-Hill Higher Education: New York, 2002; p 467.

and CO. Unburned hydrocarbon and particulate emissions in Stirling burners are negligible compared to those in IC engines.[2]

Various authors have studied Stirling engines for power applications. Hoagland et al.[4] have characterized the emissions of the diesel-fueled United Stirling P-75 heavy duty truck engine, a 75 kW four-cylinder double-acting system with twin cranks and parallel cylinders arranged in a square. This engine runs on helium pressurized to 14 MPa and exhibits a maximum energy efficiency of 37% under laboratory conditions when fueled by hydrogen. They claim that emissions of all species are lower than for diesels and gas turbines with $0.67-2.68$ g/(kW h) of NO_x, $0.67-2.68$ g/(kW h) of CO, and $0.01-0.07$ g/(kW h) of unburned hydrocarbon (UHC) emissions.

Bennethum et al.[5] have performed extensive testing of the STM4-120 engine manufactured by Stirling Thermal Motors, Inc. (STM). This system is a four-cylinder and double-acting engine optimized to output 25 kW of power. This engine runs on helium working fluid and is designed to operate on a variety of fuels. Emission data are, however, only available for natural gas and diesel. For natural gas, and air/fuel equivalence ratios of $1.2-1.6$, the engine produces $0.07-0.17$ g/(kW h) of NO_x, $1.25-0.79$ g/(kW h) of CO, $0.29-0.34$ g/(kW h) of UHCs, and negligible particulates. For diesel, the engine produces 0.43 g/(kW h) of NO_x, 0.50 g/(kW h) of CO, 0.07 g/(kW h) of UHCs, and negligible particulates.

Bandi et al.[6] have modified a propane gas flameless oxidation (FLOX) burner and mounted it on a Stirling CHP system (SOLO 25 kW thermal). This burner is suitable for fast pyrolysis oil fueling since the residence time of the burning chamber is higher than that of normal burning for propane that aids the complete carbon burnout. For the atomization of the oil, a pressurized air atomizer with an external mixing chamber is selected. The engine produces $20-95$ mg/m^3 NO_x, $35-125$ mg/m^3 CO, $20-40$ mg/m^3 UHCs, and negligible particulates.

1.3. Biodiesel. Many countries are considering alternatives to imported petroleum. Currently, there is a growing interest in the use of biodiesel, derived from vegetable oils or animal fats, as a renewable replacement (pure or blended) for petroleum-based diesel in transportation, heating, and electricity generation.[7,8] ASTM International defines biodiesel as "a fuel comprised of mono-alkyl esters of long chain fatty acids derived from vegetable oils or animal fats, designated B100, and meeting the requirements of ASTM D6751". The advantages of using biodiesel are that it can be renewable, locally produced, less polluting, and more biodegradable and can support the rural economy and reduce net greenhouse gas emissions.[7,8] However, it has a number of physical and chemical properties that can make it difficult to use such as a narrower evaporation range, higher evaporation temperatures, a higher oxygen content, and a higher viscosity.[7,8]

Biodiesel has been extensively tested in internal combustion engines. In their review paper, Lapuerta et al.[9] found that, in general, engines running on biodiesel had a thermal efficiency

(4) Hoagland, L. C.; Percival, W. H. *Proceedings of the 13th Intersociety Energy Conversion Engineering Conference*; Society of Automotive Engineers: San Diego, CA, 1978; pp 1865–1871.

(5) Bennethum, J. E.; Laymac, T. D.; Johansson, L. N.; Godett, T. M. *SAE Tech. Pap. Ser.* **1991**, 1–5.

(6) Bandi, A.; Baumgart, F. *Proceedings in Thermochemical Biomass Conversion*; Blackwell Publishing: Oxford, U.K., 2001; Vol. 2, pp 1459–1467.

(7) Kinast, J. A. *Production of Biodiesels from Multiple Feedstock and Properties of Biodiesels and Biodiesel/Diesel Blends*; NREL/SR510-31460; NREL: Des Plaines, IL, 2003.

(8) Demirbas, A. *Prog. Energy Combust. Sci.* **2007**, *33*, 1–18.

(9) Lapuerta, M.; Armas, O.; Rodriguez-Fernandez, J. *Prog. Energy Combust. Sci.* **2008**, *34*, 198–223.

Figure 1. Whispergen DC system.

Table 1. Whispergen DC System Specifications

feature	specifications
prime mover	four-cylinder double acting
power output	0.8 kW nominal
heat output	5.5 kW nominal
fuel	no. 2 diesel
consumption	maximum 1 L/h
exhaust	475 °C
size	$450 \times 500 \times 650$ mm^3

similar to that of conventional diesel and particulate, total UHC, polyaromatic hydrocarbon (PAH), and CO emissions much lower than those of conventional diesel. They suggest the reduction in particulates is due to the biodiesel's oxygen content and its absence of aromatics; biodiesel's oxygen content is responsible for the more complete combustion. However, engines running on biodiesel had a slight increase in NO_x emissions due to the injection process being slightly advanced. They suggest that this could be remedied by a delay in the fuel injection.

1.4. Objectives. Although biodiesel has been extensively tested in compression ignition engines, the authors have found no literature that uses biodiesel in external combustion heat and power devices such as the Stirling engine. In low-power applications, the Stirling engine offers competitive energy efficiency in the conversion of fuel energy into heat and power. The focus of the current research, therefore, is to compare the performance of a Stirling-engine-based microcogeneration system using no. 2 diesel fuel and biodiesel by performing energy analysis, as well as particulate, unburned hydrocarbon, CO, NO_x, and aldehyde emissions tests.

2. Experimental Section

2.1. Stirling Engine CHP system. WhisperGen, a New Zealand firm, manufactures micro-CHP systems. The combustion group at the University of Toronto has acquired a diesel-fuel-fired Whispergen micro-CHP system and has carried out energy performance and emission testing of this system fueled by diesel and biodiesel. The system integrates a burner, a Stirling engine, a generator, and a controller in a compact assembly. This system is shown in Figure 1, and the specifications are shown in Table 1.

The burner features a continuous combustor with a single swirl evaporator that provides heat to the engine. Thus, the fuel is not directly injected as a spray but rather first enters an evaporator and then is mixed with air. The engine has a four-cylinder α-type double-acting arrangement that is hermetically sealed for prolonged

Figure 2. Whispergen DC system installation.

periods of operation. Carlgvist et al.[10] provide the operating characteristic of α-type double-acting Stirling engines. Nitrogen is the working fluid inside the engine and is pressurized to 28 bar. For this engine, Clucas et al.[11] report a displacement of about 101 cm³ (4 cm bore, 2 cm stroke) and a shaft speed of 1200−1500 rpm. The pistons are made of alloy steel and run in filled PTFE lip seals backed with O-rings. The engine's internal heat exchangers (regenerators) are made out of copper. The DC Whispergen provides 12 V of DC power.

Figure 2 shows the Whispergen DC CHP system as it is installed in the laboratory for testing. An Interstate 216 Ah deep cycle battery is used to load the electrical output of the generator. The electricity recharged in the battery is also converted to 120 V of AC power using a Xantrex 1000 W inverter. A Seakamp copper shell-and-tube heat exchanger is used to load the thermal output. This heat exchanger removes heat from the system by running cold tap water through the shell. The engine coolant passes through tubes in a counterflow arrangement. The cooling system consists of a coolant pump and a header tank.

The fuel is supplied from a 2 L graduated bottle via a pulsed fuel pump, and the fuel consumption rate is measured by reading the graduated bottle to within 10 mL accuracy. An Eldridge air mass flow meter is used to measure the intake air to 5 L/min accuracy. The CHP system is also equipped with various sensors, outputs of which are logged by a computer. These outputs include the glow plug operation, fuel supply rate, air supply rate, engine power output, exhaust temperature, ceramic temperature, coolant temperature, and more. This software not only provides the capability to observe and log the engine performance, but also enables the user to adjust various engine operating parameters for optimum performance.

The system can be run in either the heat-manage mode or the autocharge mode. In heat-manage mode, a constant coolant temperature is maintained, and hence, thermal energy is transferred from the system to the load. In autocharge mode, the engine runs until the battery is charged, after which point the system automatically shuts down. In other words, the former operating strategy uses heat demand as the controlling parameter to turn the system on or off, whereas the latter operating strategy uses electricity demand as the controlling parameter.

For all diesel and biodiesel tests, the microcogeneration system is run in heat-manage mode for 1 h. This time period is representative of the system operating in a real life application. During this time interval, the system goes through several operating stages of preheating, running up, running (steady-state), running down, and

(10) Carlgvist, S. G.; Göthberg, Y. *Proceedings of the 24th Intersociety Energy Conversion Engineering Conference*; Institute of Electrical and Electronics Engineers: Washington, DC, 1989; Vol. 5, pp 2265−2270.

(11) Clucas, D. M.; Raine, J. K. *Proc.−Inst. Mech. Eng.* **1994**, *208*, 357–365.

Table 2. Fuel Properties of Standard No. 2 Diesel and Animal Fat Biodiesel

property	test method	diesel	biodiesel
heat of combustion at 2500 °C (MJ/kg)	ASTM D4809	42.792	42.840
90% distillation temperature (°C)	ASTM D86 ASTM D1160	290.5	350.0
chemical makeup, C−H−O (mass %)	ASTM D5291	86−13−0	76−13−11
kinematic viscosity at 4000 °C (mm²/s)	ASTM D445	1.930	4.534

cooling off. In practice, the system can be operated at longer time intervals as long as heat and/or electricity are demanded. A longer operation time interval does not require a cyclic start-up and shut-down of the system; instead, it simply extends the running (steady-state) stage.

The glow plug operation is controlled using the burner temperature as a feedback parameter. The fuel supply rate is controlled such that the exhaust temperature is maintained at a set point of 480 °C. The amount of air provided for combustion is controlled by an O_2 sensor to maintain a fixed fuel/air equivalence ratio. The Whispergen burner is usually operated in a fuel lean situation primarily to reduce the NO_x emissions. The engine is operated until the temperature of the coolant reaches a set point of 70 °C, at which point it stops. For continued operation, however, the coolant is cooled by the external heat exchanger to avoid a premature shutdown.

Various important operating parameters will affect the system performance: The glow plug start-up heating duration helps stabilize the flame and warm the burner. However, since it consumes 400 W of power, extended glow plug heating will cause a net decrease in the power output of the system. The fuel supply rate determines the total heat input to the system and strongly affects the exhaust temperature. The fuel/air equivalence ratio affects the flame and burner temperature. With higher fuel/air equivalence ratios, the burner operates at higher temperatures that may overheat the system components and/or eventually disturb the flame stability.

2.2. Fuel Properties. A study by Kinast at the National Renewable Energy Laboratory (NREL)[7] reveals the biodiesel properties that most commonly affect the engine performance. These are the heating value (measure of the fuel energy content), distillation temperature (fuel volatility), chemical makeup (carbon, hydrogen, and oxygen content), and viscosity (fuel flow characteristics). Table 2 shows these important properties for the diesel and biodiesel fuels tested in the present study. The biodiesel used is derived from animal feedstock and is provided by Rothsay.

The two diesel and biodiesel fuels have similar heats of combustion. Biodiesel, however, evaporates at a higher range of temperatures. Also, the biodiesel under study is oxygenated and exhibits a higher viscosity than standard no. 2 diesel.

2.3. Energy Efficiency. Energy efficiency gives the ratio of utilized energy in the form of heat and power to the input energy. Energy efficiency can be obtained by using the following equation:

$$\eta_{energy} = \frac{\dot{W} + \dot{Q}}{\dot{m}_F h_F} \qquad (1)$$

where $\dot{W}$ is power, $\dot{Q}$ is recovered heat, $\dot{m}_F$ is the fuel mass flow rate, and h_F is the fuel specific enthalpy. In the present study, $\dot{Q}$ refers to the useful form of heat that is recovered by heat exchangers only. Any form of heat loss is not captured and, consequently, not included in $\dot{Q}$. Note that, in this equation, the energy input is the total heating value of the fuel.

2.4. Particulate Emissions. Diesel exhaust particulate matter causes many kinds of health problems such as asthma, persistent bronchitis, and lung cancer. For particulate collection, direct isokinetic sampling of the exhaust is made. The particulate concentration in the exhaust is determined from the mass collected on a filter and the exhaust flow rate. Agglomerate sizing is
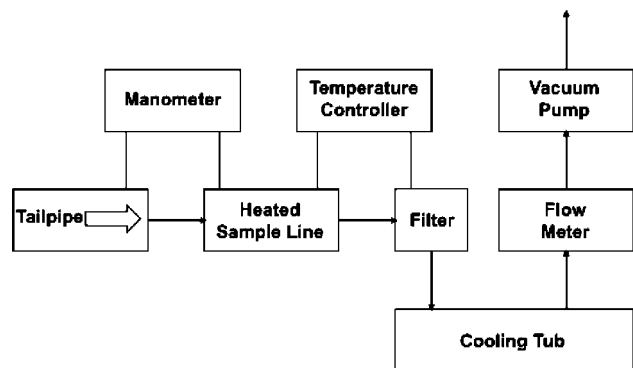
Figure 3. Direct particulate sampling schematic.

determined by a simple method devised by Vuk et al.[12] called "the largest sphere method" where the soot particle size is quantified with the smallest diameter of a sphere which can contain the entire agglomerate.

The particulate collection setup is shown schematically in Figure 3. A tapered and machined aluminum probe is used to draw the sample from the exhaust. The probe features a sharp edge to minimize disturbance of the flow. The system also features a heated line before the filter so that the sample exhaust is maintained at 50 °C using a temperature controller and a feedback thermocouple. The setup also features a cooling tub, a coalescent water filter, a flow meter, and a vacuum pump. Particulates are collected on Pall EMFAB filters that provide 99.99% retention for particulate sizes larger than 0.3 μm. The filter weights are measured before and after particulate collection using an Ohaus Analytical Plus microbalance. They are further viewed under a Buehler Micromet 2101 optical microscope and a Hitachi S-5200 scanning electron microscope.

2.5. Unburned Hydrocarbon Emissions. The United States Code of Federal Regulations (CFR) has also recommended a procedure (86.1310-2007) to evaluate the total hydrocarbon emissions from diesel engines. A typical instrument used for total unburned hydrocarbon emission is the flame ionization detector (FID). In this method, the hydrocarbons present in the exhaust sample are burned in a small hydrogen-air flame that produces ions proportional to the number of carbon atoms in the exhaust. The carbon rule states that the amount of current produced is directly proportional to the number of carbon atoms ionized; hence, the FID is essentially a carbon atom counter.[13]

The California Analytical model 600 HFID heated total hydrocarbon analyzer is used to measure the total amount of UHC emissions in the exhaust. Figure 4 shows a schematic of the test setup. The HFID is calibrated with sample gases that contain the minimum and maximum concentrations of hydrocarbons for the range of detection. The concentrations are reported as mole fraction in parts per million of methane (CH_4). A heated filter is used to filter any particulates that are present in the exhaust. A Pacwill Environmental heated filter and a Unique Heated Products heated transfer line with feedback temperature controllers are used to maintain the temperature of the exhaust at 196 °C from the point of sampling to the HFID analyzer.

2.6. Exhaust Species Measurement. Carbon monoxide, nitric oxide, nitrogen dioxide, methane, acetylene, ethylene, formaldehyde, and acetaldehyde in the exhaust have been measured with a Nicolet 380 Fourier transform infrared (FTIR) spectrometer with a resolution of 1 cm^{-1}. By comparing the spectrum of an unknown sample to the spectrum of known standards, it is possible to determine what components, and with what concentrations, are present in an unknown sample. In the present analysis, a partial least-squares (PLS) calibration model is used.[18]

Figure 5 shows a schematic of the test setup. The exhaust gas must be sampled and delivered to the spectrometer at a fixed

(12) Vuk, C. T.; Jones, M. A.; Johnson, J. H. *Measurement and Analysis of the Physical Character of Diesel Particulate Emissions*; SAE Preprints 760131; SAE: Warrendale, PA, 1976.

(13) Heywood, J. B. *Internal Combustion Engine Fundamentals*; McGraw-Hill, Inc.: New York, 1988; pp 145−146.
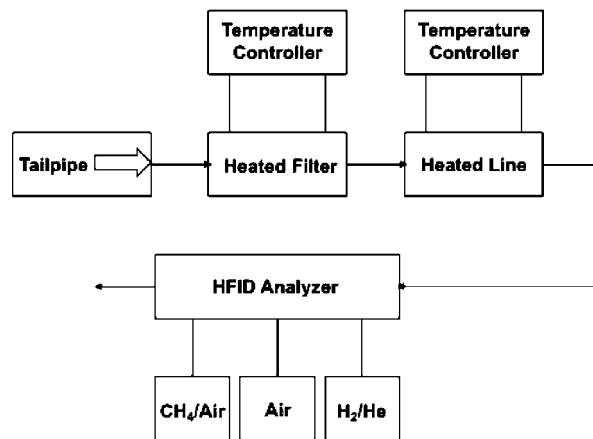
Figure 4. HFID sampling schematic.
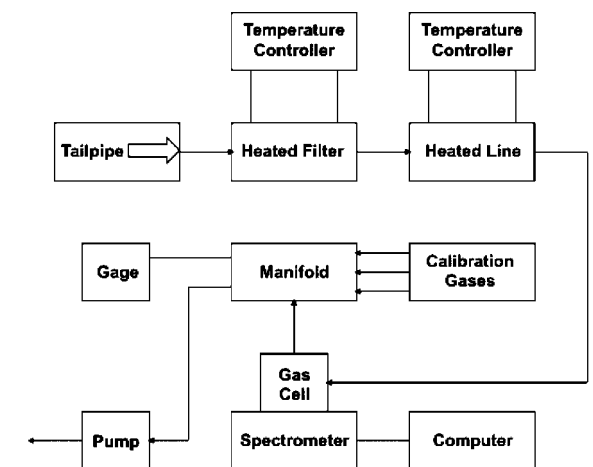
Figure 5. FTIR test setup schematic.

Table 3. Whispergen DC System Performance

fuel	fuel flow (L/m)	power (kW)	heat (kW)	power efficiency (%)	heat efficiency (%)	total efficiency (%)
diesel	0.0160	1.11	7.44	11.7 ± 0.06	78.7 ± 0.23	90.5 ± 0.24
biodiesel	0.0155	1.11	7.51	11.5 ± 0.06	77.5 ± 0.23	89.0 ± 0.24

temperature and pressure (100 °C and 86.3 kPa A) to ensure experiment repeatability. To maintain the temperature of the exhaust, the same heated filter and heated transfer line are used as in the HFID setup.

3. Results and Discussion

3.1. Energy Efficiencies. Table 3 shows the DC Whispergen system performance in rated steady-state operation fueled by diesel and biodiesel. The efficiencies are calculated on the basis of the lower heating value (LHV). The power and heat efficiencies are each measured three times, and from this data, the standard errors are calculated to be 0.06% and 0.23%, respectively (SE = $S/N^{1/2}$, where SE = standard error, S = sample standard deviation, and N = number of measurements). The total efficiency is the sum of the power and heat efficiencies with a standard error of 0.24%. This error propagation is obtained by adding the power and heat efficiency errors in quadrature [$SE_{total} = (SE_{power}^2 + SE_{heat}^2)^{1/2}$].

The efficiencies are expected to be close since the heat of combustion for diesel (42.79 MJ/kg) is close to that of biodiesel (42.84 MJ/kg). Therefore, the fuel chemical composition does not make a large difference in the amount of heat release. However, the slight difference in efficiency can be understood

Table 4. Whispergen DC System Particulate Emissions

fuel	net mass (mg)	particulate emissions (mg/m^3)	particulate emissions index [mg/(kW h)]
diesel	1.40 ± 0.04	0.65 ± 0.02	2.33 ± 0.07
biodiesel	37.88 ± 0.1	21.35 ± 0.05	69.21 ± 0.18

when considering the fuel properties. The boiling temperature range for biodiesel is higher than that of diesel (Table 2). Therefore, a small fraction of the biodiesel is not evaporated and burned, resulting in a slightly lower efficiency of the system when run on biodiesel. The total energy efficiencies are high since Whispergen features a highly effective heat recovery system that captures most of the excess heat in the exhaust.

3.2. Particulate Emissions. Since the Whispergen burner features a continuous premixed flame, proper fuel evaporation plays a critical role in the complete burnout of the fuel and therefore particulate emissions. Table 2 shows a lower distillation temperature for the diesel (290.5 °C) than for the biodiesel (350.0 °C) used in this study; therefore, a higher fraction of fuel is expected to remain unevaporated for biodiesel. The flame temperature is not available from the data logged by the engine, but the burner temperature is the next closest measure in understanding fuel evaporation. The burner temperature is measured to be 425 ± 5 °C at the hottest surface that is on top of the cylinders. This temperature is lower than that of compression ignition engines, explaining that more particulate emissions are likely to form due to incomplete fuel evaporation.

Table 4 shows the exhaust particulate emissions collected on the diesel and biodiesel filters. The weight for each filter is measured three times before and after the particulate collection. Again using the error propagation principle, the standard error for the net filter weight is 0.04 mg for diesel and 0.1 mg for biodiesel. The standard errors for the net filter weights in other units are simply scaled to be 0.02 mg/m^3 and 0.07 mg/(kW h) for diesel and 0.05 mg/m^3 and 0.18 mg/(kW h) for biodiesel.

The low particulate emissions for diesel are expected since the burner features a continuous flame that facilitates the complete burnout of already evaporated diesel fuel in a premixed combustion. Compared to those of diesel, relatively higher particulate emissions for biodiesel are observed. This is in agreement with Kinast's study[7] that suggests a higher boiling point for most compounds results in a substantial amount of unevaporated fuel in the exhaust.

Figures 6 and 7 show pictures of the particulates collected on the Pall EMFAB filter using the Hitachi S-5200 scanning electron microscope for the diesel and biodiesel tests. Clear differences are observed between the two. The diesel filter appears as gray, and the SEM picture of this filter shows agglomerates on one strand of the filter. These observations
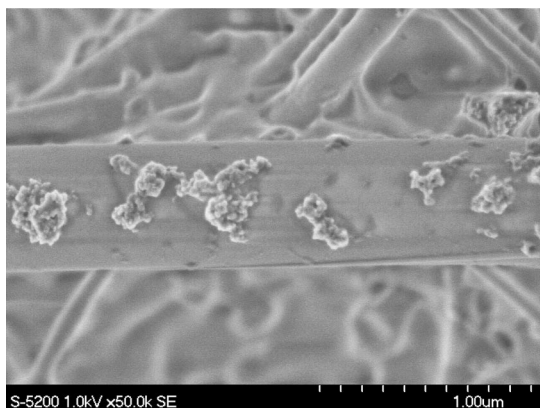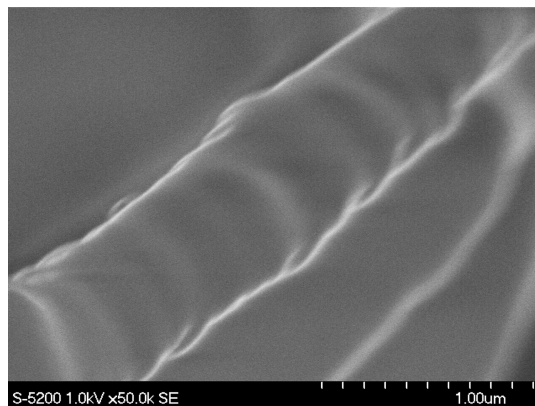
Figure 7. SEM image of filter paper from the biodiesel test.
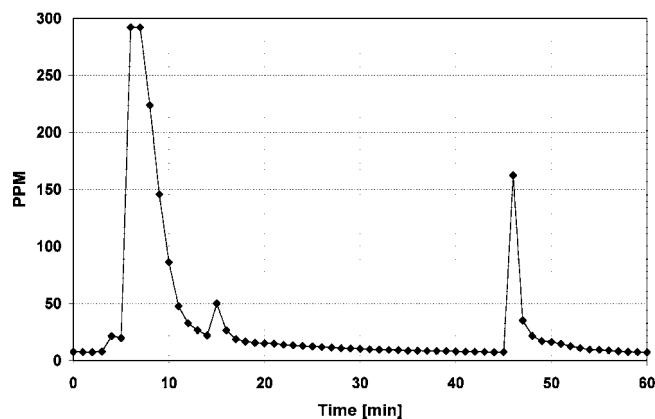
Figure 8. Diesel total UHC emissions.

suggest that what is seen on the filter is primarily soot. On the other hand, the biodiesel filter appears as light amber and the SEM image shows a smooth and continuous deposit of matter on one strand. These observations suggest that a significant amount of unevaporated fuel is deposited on the filter.

3.3. Unburned Hydrocarbon Emissions. The California Analytical model 600 HFID heated total hydrocarbon analyzer measures the total amount of UHC emissions in the exhaust with an uncertainty of 1 ppm. Figure 8 shows the total diesel UHC emissions for a 1 h test duration. The sampling frequency is 1 min to show the system's transient behavior. During the start of the preheating stage (0−5min), there are low UHC emissions of less than 8 ppm. This is due to the heating of the evaporator by the glow plug, which in turn results in incomplete burning of any fuel deposits at the vicinity of the heat source. After the fuel injection and production of the flame (5−14 min), the UHC emissions reach a maximum saturation value of 292 ppm and drop to 22 ppm as the flame stabilizes. At this point the glow plug is turned off and the flame will sustain itself by the heat radiation from the internal surfaces of the combustion chamber. This occurs concurrently with the Stirling engine running up. During a short period (14−20 min), the UHC emissions rise to 50 ppm because the glow plug is not on anymore. This peak, however, ends after a short period of time, and the UHC emissions continue to drop to 7 ppm as the engine reaches the end of the running stage (20−45 min). At running down (45−50 min) and upon the termination of the flame, the UHC emissions rise one more time to 162 ppm and then fall to 7 ppm by the end of the cooling off stage (50−60 min). The presence of the UHC emissions even after the flame extinction can be attributed to the incomplete burning of fuel deposits on combustion chamber surfaces.

Figure 6. SEM image of filter paper from the diesel test.
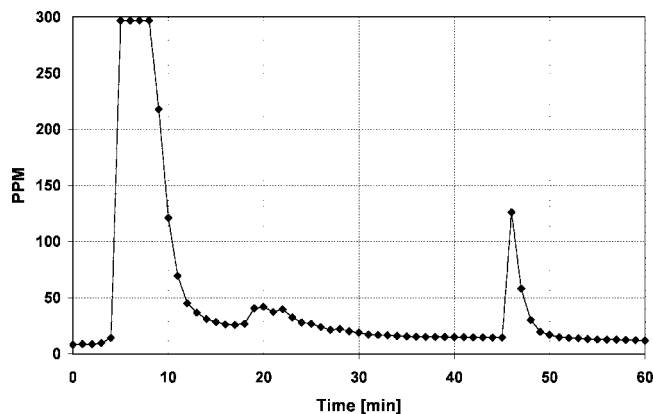
Figure 9. Biodiesel total UHC emissions.

Figure 9 shows the total biodiesel UHC emissions for a 1 h test duration. The system operation stages follow the same sequence for biodiesel; however, the timing for each sequence can be different. During the start of the preheating stage (0−5 min), there are low UHC emissions of less than 9 ppm just like the diesel case. However, the flame stabilization for biodiesel takes longer (5−18 min). This is, again, due to biodiesel's higher boiling range. To tackle this problem, the glow plug operation is extended an extra 4 min to facilitate the preheating stage. A second peak in UHC emissions (42 ppm) is observed when the glow plug is turned off (18−24 min). This transient effect ends, and the UHC emissions drop to a value of 14 ppm by the end of the running stage (24−45 min). Similar to diesel, the UHC emissions peak at 126 ppm when the flame is extinguished with the engine running down (45−50 min). The UHC emissions continue to drop to 12 ppm by the end of the cooling off stage. Overall, the biodiesel UHC emissions are observed to be higher than those of diesel. This may seem contrary to other studies[14,15] performed on internal combustion diesel engines fueled by B20, but the Whispergen engine operates on the basis of evaporating the fuel for a premixed combustion flame. Since biodiesel is more difficult to evaporate due to the higher boiling range, the high UHC emissions are in line with expectations.

3.4. Exhaust Species Measurement. The sampling frequency for the Nicolet 380 FTIR spectrometer is set to 1 min with 24 scans for each reading to predict species concentrations. PLS analysis enables concentration measurements of all species in the range of 10−250 ppm with an uncertainty of less than 7 ppm.

The diesel emissions measured by the Nicolet 380 FTIR spectrometer are shown in Figure 10. During the preheating stage (0−5 min), there is a trace amount of CO due to incomplete burning of any fuel deposits on the burner internal surfaces. In this stage, however, other pollutant species are present below the spectrometer's detection limit. At the start of the fuel injection and flame stabilization (5−14 min), most pollutants reach their maximum level, except for NO and NO_2. At this stage, the prevalent pollutants are CH_2O (121 ppm), C_2H_4 (106 ppm), CO (99 ppm), C_2H_4O (67 ppm), CH_4 (33 ppm), C_2H_2 (13 ppm), and NO_2 (10 ppm). Subsequently, in the running up and running stages (14−45 min), the NO and NO_2 emissions reach 151 and 25 ppm, respectively. This is expected since the dominant mechanism for NO_x formation is thermal NO_x, which

(14) United States Environmental Protection Agency (U.S. EPA). EPA420-P-02-001; Washington, DC, 2002.

(15) Durbin, T. D.; Cocker, K.; Collins, J. F.; Norbeck, J. M. *Evaluation of the Effects of Biodiesel and Biodiesel Blends on Exhaust Emission Rates and Reactivity*−2; College of Engineering, University of California: Riverside, 2001.
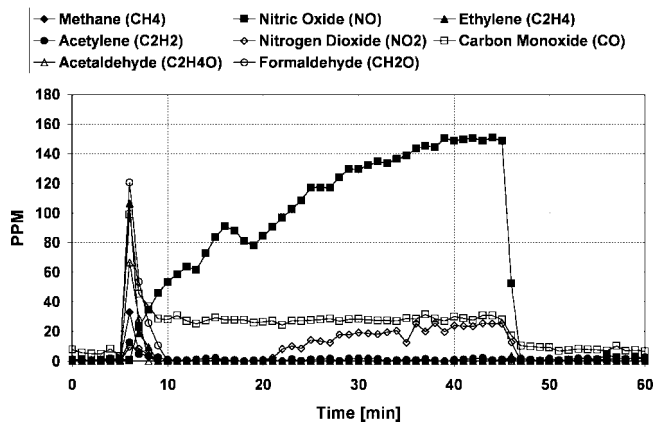
Figure 10. Diesel FTIR emissions.
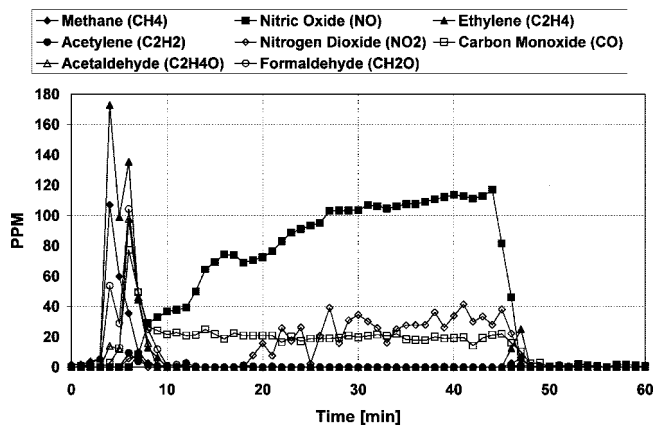
Figure 11. Biodiesel FTIR emissions.

increases as the burner temperature rises. The CO emission level remains approximately constant below 27 ppm during the running up and running down stages. At running down and cooling off (45−60 min), most pollutants are present below the detection limit. During these stages, there is a trace amount of CO below 10 ppm.

The biodiesel emissions measured by the Nicolet 380 FTIR spectrometer are shown in Figure 11. Similar to diesel emission, during the preheating stage (0−5 min), most pollutant species are present below the spectrometer detection limit. At the start of the fuel injection and flame stabilization (5−18 min), however, most pollutants reach their maximum level, except for NO and NO_2. At this stage, the prevalent pollutants are CH_2O (104 ppm), C_2H_4 (173 ppm), CO (77 ppm), C_2H_4O (98 ppm), CH_4 (107 ppm), C_2H_2 (9 ppm), and NO_2 (6 ppm). Compared to those of diesel, the above emission levels are in the same order; however, the flame stabilization for biodiesel takes longer due to its higher fuel boiling point temperature range. To assist the preheat process, the glow plug operation is extended for an extra 4 min. Subsequently, in the running up and running stages (18−45 min), the NO and NO_2 emissions reach 117 and 42 ppm, respectively. Compared to that of diesel, a lower amount of NO emissions is observed, which is consistent with the EPA study[14] as it was found that NO_x emissions from animal-fat-based biodiesel are less than those of standard diesel. It is suggested that the higher boiling point compounds that do not evaporate cause local wall quenching effects that can lower the flame temperature at locations and, hence, reduce thermal NO_x. During running down and cooling off (45−60 min), most pollutants are present below the detection limit.

3.5. Sensitivity Analysis. The Whispergen system is designed to run on standard no. 2 diesel and not biodiesel. This

Table 5. Sensitivity Test Conditions

air flow (SLPM)	fuel to air equivalence ratio	burner temp (°C)
300.9	0.52	454.0
273.5	0.57	458.8
243.1	0.64	463.9
216.9	0.71	480.0
185.2	0.84	489.0

brings up the following question: What mechanisms are responsible for the emission differences, if any, when the system is run on biodiesel instead of diesel? A sensitivity study helps answer this question. A useful sensitivity analysis is to change the biodiesel fuel/air equivalence ratio by keeping the fuel flow rate constant and by varying the air flow rate.

To perform this study, the engine is started as usual to reach steady-state performance, reaching a constant exhaust temperature and outputting the rated electricity and thermal power. At this point, the engine control software is used to vary the air flow rate while keeping the fuel flow rate constant (16.4 mL/min) to achieve different fuel to air equivalence ratios, from the lowest to the highest. Table 5 shows the air flow rate, biodiesel fuel to air equivalence ratio, and burner temperature test conditions for the sensitivity test.

The most important outcome of the sensitivity test is the FTIR spectroscopy emissions results. Figure 12 shows how the emissions are affected by varying the fuel to air equivalence ratio. It is observed that the CO emissions increase from a low level of 17 ppm to a high level of 38 ppm. This is expected since, as the equivalence ratio increases, the amount of excess air decreases. The NO_2 emissions are seen to increase from a low level of 25 ppm to a high level of 42 ppm. The most sensitive pollutant to the equivalence ratio (or alternatively the exhaust temperature) is NO. For the range of air flow rates in Table 5, NO emissions are observed to be at 82, 108, 138, 207, and 209 ppm levels. The increasing trend in NO_x emissions confirms the hypothesis that the dominant mechanism for NO_x emissions in biodiesel is thermal.

4. Comparison with Other Residential Cogeneration Systems

Depending on the type of technology used, the energy efficiency, emissions, maintenance, noise, and cost for other cogeneration systems can be different from those of the DC Whispergen CHP system. There are many residential natural gas and diesel-based cogeneration systems in the same power range as the Whispergen system.

4.1. Energy Efficiency. Table 6 shows the energy efficiency of various micro-CHP systems based on Stirling engines, internal
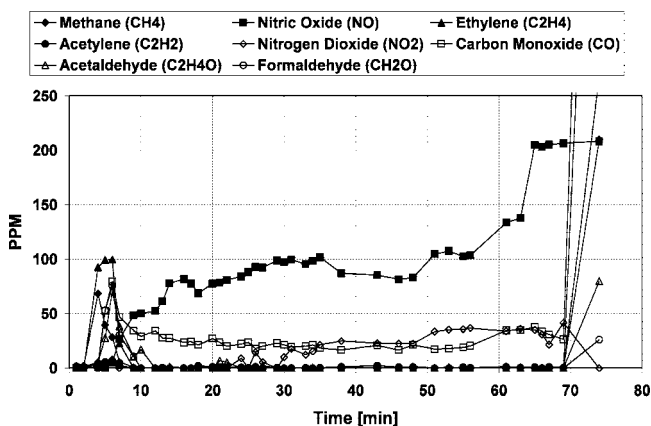
Figure 12. Biodiesel sensitivity FTIR emissions.

Table 6. Microcogeneration Efficiencies (LHV)[a]

cogeneration system	power energy efficiency (%)	heat energy efficiency (%)	total energy efficiency (%)
AC Whispergen Stirling engine (natural gas)[16]	8.5	59.9	68.4
DC Whispergen Stirling engine (diesel)	11.7	78.7	90.5
DC Whispergen Stirling engine (biodiesel)	11.5	77.5	89.0
FreeWatt SI−IC engine (natural gas)[16]	22.9	62.1	85.0
EBARA-Ballard fuel cell (natural gas)[16]	33.0	50.0	83.0
SenerTec HKA HR 5.3 CI−IC engine (diesel)[17]	30.0	59.0	89.0
SenerTec HKA HR 5.3 CI−IC engine (biodiesel)[17]	30.0	59.0	89.0

[a] SI = spark ignition, CI = compression ignition, and IC = internal combustion.

combustion engines, and fuel cells. Whispergen also manufactures a natural gas Stirling engine capable of producing 0.85 kW of electrical power and 6.00 kW of thermal power. The FreeWatt spark ignition (SI) internal combustion (IC) engine is a residential micro-CHP system developed by Honda and Climate Energy. This system runs on natural gas and provides 1.20 kW of electrical power and 3.26 kW of thermal power. The EBARA-Ballard micro-CHP fuel cell produces 1.00 kW of electrical power and 1.52 kW of thermal power.[16] The Germany-based company SenerTec has developed a compression ignition (CI) internal combustion diesel-engine-based cogeneration system suitable for a single-family residential application producing 5.30 kW of electrical power and 10.40 kW of thermal power. This system operates on both fuel oil and biodiesel.[17] In general, IC engines and fuel cells exhibit higher power energy efficiencies since IC engines operate at higher pressures and temperatures, and the fuel cells rely on an electrochemical reaction to convert power. On the other hand, the heat recovery system for all of these systems is effective such that the total energy efficiency is comparable among all of the systems.

4.2. Maintenance. The DC Whispergen CHP system requires minimal maintenance. The engine is oil-free and has low wear mechanisms. The operating engine−generator compartment is sealed so that the working fluid cannot easily leak out. The service intervals are 5000−8000 h. The nitrogen working fluid, however, needs to be refilled every 1000 h.

Reciprocating internal combustion engines require frequent inspections, service, and adjustments. The engine oil, coolant, and spark plugs are required to be changed every 500−2000 h. Also, the manufacturers recommend a top-end overhaul every 12000−15000 h and a major overhaul every 24000−30000 h. A top-end overhaul requires a cylinder head replacement, and a major overhaul requires piston, ring, crankshaft bearing, and seal replacement.

Although fuel cell systems do not have as many moving parts as the heat engines, they require frequent maintenance and some component replacement that can be costly. Fuel cells require minor maintenance together with pumps and fan replacement. A major overhaul requires catalyzer, reformer, and stack replacement. Stack replacement is expected every 4−8 years. Periodic filter replacement is carried out every 2000−4000 h.[2]

(16) Aliabadi, A. A.; Wallace, J. S.; Thomson, M. J. *Efficiency Analysis of Natural Gas Residential Micro Cogeneration Systems*; Mechanical and Industrial Engineering, University of Toronto: Toronto, 2008.
(17) SenerTec Technical Data−Dachs. http://www.senertec.de/show_pdf_en.php?name=4798_092_107_technical_data (accessed Sept 15, 2008).

4.3. Infrastructure. Any new technology must be supported by a new or existing infrastructure. For residential cogeneration technologies, the most important infrastructures are the ability to recover heat, the availability and delivery of fuel, and the capacity to use power. Most residential spaces can be retrofitted for cogeneration. This is true since the conventional furnace or hot water heater can be replaced by a cogeneration system and the water tank, controls, and the duct works can be adapted to work with the cogeneration device.

On the other hand, the fuel supply and the capacity to use power pose more difficulties. Cities often have a natural gas pipeline infrastructure that could provide the fuel for natural-gas-based cogeneration technologies. However, fuel storage tanks are necessary to provide the fuel for fuel-oil-based cogeneration systems. The fuel-oil-based cogeneration technologies are attractive in rural areas since fuel oil is usually shipped to such places and is the only source of energy.

To be able to use the power produced from these cogeneration systems, a house needs to provide its own battery bank or net meter its electricity with the grid. If the grid net metering is desired, the network must have the capacity to support it. Also, jurisdictions should facilitate the technical and economical frameworks for home owners to show interest in installing a cogeneration system.

4.4. Load Response. An important feature of a cogeneration system is its ability to respond to the power load. Internal combustion engines and fuel cells exhibit instant load response since the power unit can be run to produce electricity on demand. Also, they have the ability to operate at partial load. On the other hand, the Whispergen cogeneration system requires an initial preheating time for the burner to reach a temperature high enough to run the Stirling engine. Furthermore, the Stirling engine is always run at a constant speed to produce the rated amount of power so that it cannot operate at partial load. This is a major drawback that can be solved by net metering or using batteries.

4.5. Cost. Many decision makers consider the cost of a technology as the ultimate factor. In general, the cost of IC technology is lower than that of other technologies as it has evolved and benefited from mass production in the past century. The Stirling engines have become more cost-effective in the recent decades and have a cost comparable to that of the IC engines.[2] The fuel cell technology is, however, much more expensive and requires more development and commercialization to be competitive with the other technologies.

5. Conclusions

In this study we examined the performance of the Whispergen CHP system fueled by diesel and biodiesel. As the system was originally designed to run on diesel, proper adjustments and modifications were performed to run the system on biodiesel. An energy balance test was performed for each fuel, and the energy efficiencies were calculated. Run on diesel, the system achieved a power efficiency of 11.7% and a heat efficiency of 78.7% for a total energy efficiency of 90.5%. The corresponding efficiencies for the system, when run on biodiesel, were slightly lower at 11.5%, 77.5%, and 89.0%, respectively. Particulate emissions for biodiesel were 69.2 mg/(kW h), an order of magnitude higher than those of diesel [2.3 mg/(kW h)]. The total unburned hydrocarbon emissions for biodiesel were higher than those of diesel. The differences in energy efficiency, particulate emissions, and unburned hydrocarbon emissions were due to a considerable fraction of unevaporated biodiesel that did not burn and was present in the exhaust. Emissions of carbon monoxide, nitrogen dioxide, methane, acetylene, ethylene, formaldehyde, and acetaldehyde were comparable between diesel and biodiesel, but nitric oxide emissions for diesel were observed to be higher at 151 ppm compared to those of biodiesel (117 ppm). It was suggested that unevaporated biodiesel fuel caused local wall quenching effects that lowered the flame temperature at locations and, therefore, reduced thermal NO_x.

Further, a comparison was made between the performance of the Whispergen systems and other residential CHP technologies such as IC engines and fuel-cell-based CHP systems. The Whispergen system had lower power efficiencies compared to IC and fuel-cell-based systems, but exhibited comparable total efficiencies due to effective heat recovery.

Stirling engines require less maintenance than IC engines and fuel cells. This makes them very attractive for residential applications. Also, recent developments in micro-CHP Stirling engine design and manufacturing have made their costs competitive with those of IC-engine-based micro-CHP technologies. The cost for fuel-cell-based micro-CHP systems is, however, much higher. Compared to internal combustion engines and fuel cells, Stirling engines exhibit a poor power load following since they require time to warm up to produce the rated power. Also, cost-effective Stirling engines do not operate at partial power load.

(18) Smith, B. C. *Fourier Transform Infrared Spectroscopy*; CRC Press, Inc.: Boca Raton, FL, 1996; pp 139−156.